Pageoph, Vol. 116 (1978), Birkhäuser Verlag, Basel

Fault and System Stiffnesses and Stick-Slip Phenomena

By RICHARD E. GOODMAN[1]) and P. N. SUNDARAM[2])

Summary – This paper discusses the influence of system stiffness on the dynamic instability of fault surfaces under laboratory conditions for a number of test modes. In conjunction with shear load stiffness, the normal load stiffness, often neglected, is shown to have a considerable effect on the stick-slip process – its presence or absence and its characteristics. Also appropriate stiffnesses are suggested for an earthquake sequence modeled as a growing dislocation.

Key words: Stiffness; Stick-slip; Rock-mechanics.

1. Introduction

The term 'stick-slip' refers here to a regular jerky motion along contact surfaces. This phenomenon has long been known (e.g. WELLS, 1929) but only recently has become the object of study with reference to earthquake source-mechanisms (BRACE and BYERLEE, 1966). In attempting to relate measured stress-drops in laboratory stick-slip experiments with the estimated stress-drops of actual earthquakes, differences in magnitude of large proportion have been a source of consternation; an order of magnitude smaller stress-drops in actual earthquakes are attributed to the action of gouge along the fault surfaces, confinement at the locked extremities of the slipping region, the influence of system stiffness, and other factors. It is with respect to the influence of system stiffness on stick-slip that this paper is mainly concerned.

Investigators of fault-dynamics have used a variety of laboratory techniques, some of which are sketched in Fig. 1. Because the independent variables differ from apparatus to apparatus, stress-drops and other observable phenomena such as amount and duration of slip vary widely in magnitude, even from one laboratory investigation to the next. BYERLEE and BRACE (1968) reported deviator stress-drops in triaxial experiments with Westerly granite of the same order of magnitude as the confining pressure, while SCHOLZ *et al.* (1972) reported shear stress-drops in biaxial experiments on the same rock type of only one-tenth of the normal stress.

In a triaxial test, a deviator stress-drop introduces changes in *both* the normal stress across and shear stress along the fault surfaces. However, in a direct shear test, where the fault is oriented parallel to the directions of shear load application,

[1]) Department of Civil Engineering, University of California, Berkeley, Cal. 94720, USA.
[2]) Department of Civil Engineering, University of Wisconsin, Milwaukee, WI, 53201, USA.

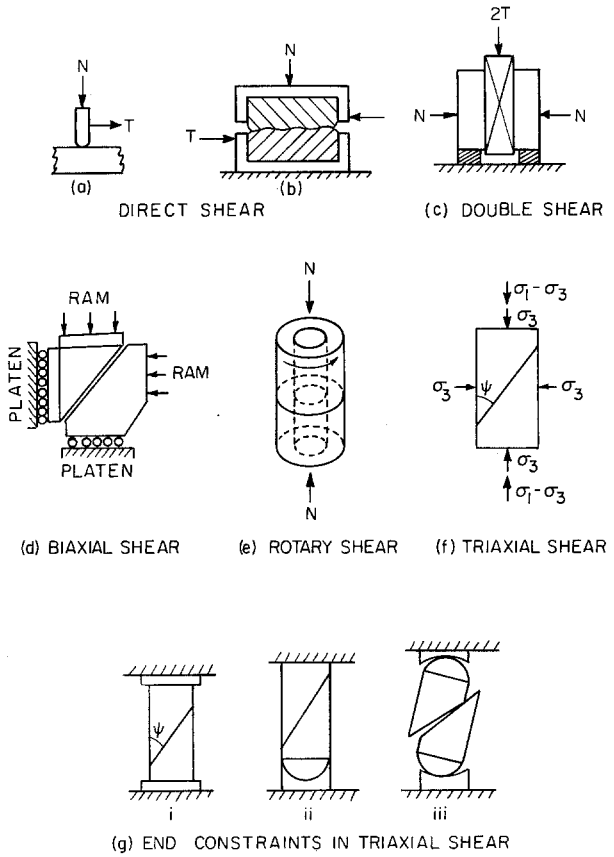

Figure 1
Laboratory techniques for sliding experiments.

the normal load remains practically constant unless the fault surfaces are very rough. It is not obvious how these various testing modes might relate to one another and to the prototype fault which is the object of observations. In this paper, therefore, we discuss how the stick-slip might be altered by changing the style of confinement and loading.

2. *Models for the different test modes*

Figure 2a shows a block of mass M on a clean, smooth fault surface of contact area A. F_y is the normal load. As the horizontal force F_x is slowly increased, the theory of friction presumes no slip occurs between the block and the supporting surface until the full frictional resistance has been mobilized. The simplest model that permits jerky motion is sketched in Fig. 2b, where the frictional resistance is assumed

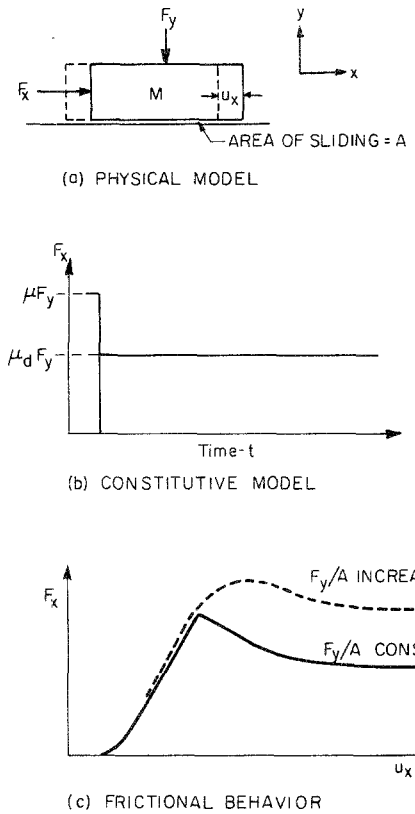

Figure 2
Sliding behavior of a block on a fault plane.

to drop immediately from a value μ to a smaller value μ_d, as soon as the force F_x reaches the magnitude μF_y. As a result, a small increment of slip produces a stress unbalance which causes the block to accelerate at a rate and for a duration dependent upon the spring constants and damping associated with the application of forces F_x and F_y. (In this discussion, damping will not be considered.)

In contrast to the model represented in Fig. 2b, actual shear tests performed in a direct shear machine on rough rock surfaces, at low normal stresses such that stable sliding prevails, reveal a shear force versus shear displacement relationship as depicted in Fig. 2c. As the force F_x is applied with an initially small force, F_y, a small slip occurs along the fault. If the stiffness associated with F_y is large, the accompanying normal deformation u_y increases the normal force and the shear force follows along the dotted curve. If the Y-direction stiffness is small, on the other hand, the normal load and thus the stress on the fault will remain practically constant[3]) and the shear

[3]) The terms normal 'stress' across and shear 'stress' along the fault indicate the applied normal or shear force divided by the gross area of the underside of the sliding block, even though the actual area of contact is much smaller.

force will follow the path of the solid line. When the peak friction has been reached, the friction drops and approaches a value sometimes called the 'residual friction'. If the stiffness of the shear loader is less than the slope of the post peak portion of the solid curve of Fig. 2c, the system becomes unstable after the peak point and the block will accelerate. It is not clear exactly what the 'dynamic friction' would be in this case, although it is possible to calculate an equivalent value based upon the simple model of Fig. 2b (BYERLEE, 1970a). The important point to be learned from Fig. 2c is that a much smaller instability or none at all should result in the case of the dotted curve. Thus, it is reasonable to conclude that the ratio of normal load stiffness to shear load stiffness must be an important control on stick-slip – its presence or absence and its characteristics.[4])

A shear force versus shear displacement relationship such as that of Fig. 2c can be attributed to formation and breaking or over-sliding of interlocks along the rough surface. A similar mechanism has been invoked by BYERLEE (1970b) on a microscale to explain stick-slip on smooth surfaces – a mechanism termed 'brittle instability'.

In order to facilitate comparison of triaxial, biaxial, direct shear and field situations, the simpler model of Fig. 2b will be assumed. Figure 3 shows idealized models relating to different styles of loading. In the triaxial test, Fig. 3a, the sliding surface is at an angle ψ with direction of load application so that slip causes the slider to move uphill, compressing the confining pressure spring k_2. The stiffness of the loader, k_1, is prescribed by the equipment and connections used. BYERLEE and BRACE (1968) used a variable-length column of water in series with the load piston to adjust the stiffness k_1 from 2×10^4 kN/m to 20×10^4 kN/m. The stiffness k_2 would be very small if a gas were used to supply the confining pressure or to serve as an accumulator for a hydraulic confining system. On the other hand, if tests were conducted inside a thick copper jacket, the stiffness k_2 would be high and the force F_y would increase during slip.

Figure 3b depicts a direct shear test on a rough fault surface, with asperities inclined at angle i with the mean plane along the fault. This test is similar to the triaxial test in that sliding occurs at an angle with respect to the applied load, since each slip must advance the slider in direction i, though the net accumulated movement will be parallel to the applied force. Again, the load stiffness k_1 is prescribed by the equipment used. Two types of direct shear machines are used – hydraulically driven machines, with relatively low stiffness, and screw-powered machines like ours, which are somewhat stiffer. Our machine has a stiffness, k_1 of 12×10^4 kN/m. The normal confinement in a direct shear machine can be applied by an external hydraulic piston, by a dead weight system with levers, or by a rigid platen; thus k_2 in practice varies from close to zero to almost infinity. Figure 3c depicts a direct shear test along polished flat surfaces aligned perfectly with the loader so that shear motion is parallel with k_1.

[4]) TOLSTOI (1967) was apparently the first to recognize the significance of the normal stiffness and normal vibrations in both stable sliding and stick-slip of metallic surfaces. OBERT *et al.* (1976) discussed the effect of normal stiffness on the shear strength of intact and fractured rocks.

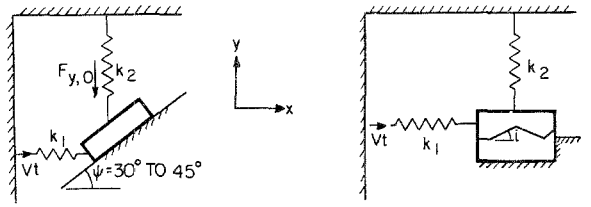

(a) TRIAXIAL TEST
(NON-DILATANT FAULT)*

(b) DIRECT SHEAR TEST
(DILATANT FAULT)
$\psi = i$ (ROUGHNESS ANGLE)

k_1 PRESCRIBED BY THE LOADING MACHINE
$k_2 \approx 0$ FOR GAS SYSTEM
$\neq 0$ FOR OIL SYSTEM WITH SLOW RESPONSE
$>> k_1$ UNIAXIAL STRAIN (NO LATERAL DISPLACEMENT)

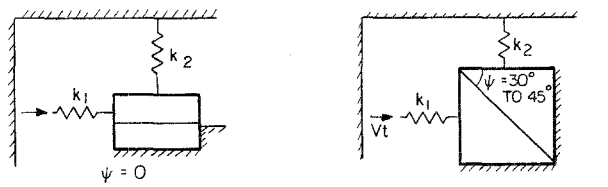

(c) DIRECT SHEAR
(NON-DILATANT FAULT)*

(d) BIAXIAL TEST
(NON-DILATANT FAULT)*
$k_1 \approx k_2$

k_1 PRESCRIBED BY THE LOADING SYSTEM
$k_2 \approx 0$ FOR GAS SYSTEM
$\neq 0$ FOR OIL SYSTEM
$>> k_1$ NO NORMAL DISPLACEMENT

* FOR DILATANT FAULT REPLACE ψ BY $\psi + i$

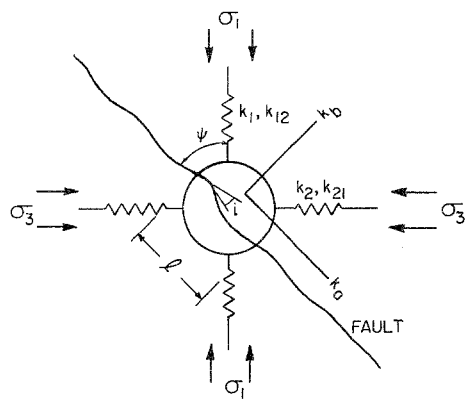

(e) PROTOTYPE FAULT

Figure 3
Models for undamped stick-slip.

Figure 3d shows a biaxial test arrangement with a fault oriented as shown. SCHOLZ *et al.* (1972) used such a device with $\psi = 30°$ while DEITERICH (personal communication) currently has a large biaxial experiment in preparation with $\psi = 45°$. The biaxial test resembles the prototype fault Fig. 3e, in which the principal stresses σ_1 and σ_3 are inclined with respect to the fault surface. In this case, the local stiffnesses parallel and normal to the fault, k_a and k_b can be transformed to direction of principal stresses to yield k_1 and k_2. In general, such a transformation also produces cross coupling coefficients $k_{12} = k_{21}$. In all the above tests, the stiffnesses k_1 and k_2 are influenced by the stiffnesses of rams, the reaction frame, and portions of the test specimen remote from the region of fault slip.

Denoting k_a and k_b as the shear and normal load stiffness referred to local coordinates, parallel and perpendicular to the fault plane respectively (Fig. 3e), the force and displacement are related by

$$\begin{Bmatrix} F_x \\ F_y \end{Bmatrix} = \begin{pmatrix} k_{11} & k_{12} \\ k_{21} & k_{22} \end{pmatrix} \begin{Bmatrix} u_x \\ u_y \end{Bmatrix} \tag{1}$$

with $k_{11} = k_a \cos^2 \psi + k_b \sin^2 \psi$

$$k_{12} = k_{21} = (k_a - k_b) \sin \psi \cos \psi$$

and $k_{22} = k_a \sin^2 \psi + k_b \cos^2 \psi$

For simplicity, the terms k_{12} and k_{21} are omitted for further analysis.

Solution to the equation of motion

For the model of Fig. 2b, the input of constant velocity V to the left end of spring k_1 in Fig. 3 yields the following equation of motion *after* the commencement of slip:

$$M\ddot{u}_x + (k_1 + \mu_d^* k_2 \tan \psi) u_x - (\mu^* - \mu_d^*) F_{y,0} = k_1 Vt \tag{2}$$

where $\mu^* = \tan(\phi + \psi + i)$; $\mu_d^* = \tan(\phi_d + \psi + i)$; and $F_{y,0}$ is the initial load in the Y direction (in spring k_2).

Let us introduce the terms, unit stiffness, $\kappa_i = k_i/A$. $(i = 1, 2)$ and the initial stress $\sigma_0 = F_{y,0}/A$. (Note σ_0 is in the Y direction, and only when $\psi = 0$ does σ_0 correspond to the normal stress across the fault above.)

The solution for the differential equation with the initial conditions $u_x = \dot{u}_x = 0$ when $t = 0$ yields

$$u_x = \frac{\mu^* - \mu_d^*}{\kappa_1 + \mu_d^* \kappa_2 \tan \psi} \sigma_0 (1 - \cos \omega t) + Vt\left(1 - \frac{1}{\omega t} \sin \omega t\right) \tag{3}$$

in which the angular frequency

$$\omega = \sqrt{A} \sqrt{\frac{\kappa_1}{M} + \frac{\kappa_2}{M} \mu_d^* \tan \psi}. \tag{4}$$

The stress drop $\Delta s = \Delta F_x/A$ and is equal to

$$\Delta s = -2(\mu^* - \mu_d^*)\sigma_0. \tag{5}$$

The *duration of slip* (t_{slip}) is

$$t_{\text{slip}} = \frac{2\Pi}{\omega} - \frac{2\tan^{-1}}{\omega}\left[\frac{\omega\sigma_0(\mu^* - \mu_d^*)}{\kappa_1 + \kappa_2\mu_d^* \tan\psi}\right]. \tag{6}$$

The *duration of stick* (t_{stick}) is

$$t_{\text{stick}} = \Delta s/\kappa_1 V. \tag{7}$$

In a direct shear test on a flat surface ($\psi = 0$), the stress-drop, $\Delta\tau$, is equal to Δs given by the equation (5), since σ_0 remains essentially constant. For $\psi \neq 0$, Δs is the drop in major principal stress, $\Delta\sigma_1$. The drop in shear stress across the fault

$$\Delta\tau = \left(\Delta\sigma_1 - \frac{\Delta F_y}{A}\right)\sin\psi\cos\psi \tag{8a}$$

and the change in normal stress

$$\Delta\sigma = \left(\frac{\Delta F_y}{A}\right) + \left(\Delta\sigma_1 - \frac{\Delta F_y}{A}\right)\sin^2\psi \tag{8b}$$

where $\Delta\sigma_1$ = the drop in major principal stress and ΔF_y is the drop in 'confining' pressure spring force. Also

$$\Delta F_y/A = (\Delta u_x \tan\psi)\kappa_2 \tag{9}$$

where

$$\Delta u_x = \Delta\sigma_1/\kappa_1, \tag{10}$$

Combining equations (9) and (10) and substituting in equation (8), we have

$$\Delta\tau = \Delta\sigma_1\left(\sin\psi\cos\psi + \frac{\kappa_2}{\kappa_1}\sin^2\psi\right) \tag{11a}$$

and

$$\Delta\sigma = \Delta\sigma_1\left(\sin^2\psi - \frac{\kappa_2}{\kappa_1}\sin\psi\cos\psi\right) \tag{11b}$$

In the triaxial test, with a gas accumulator connected to a confining liquid, $\kappa_2 \simeq 0$ and $\Delta\tau \simeq \Delta\sigma_1 \sin\psi\cos\psi$ (e.g., BYERLEE, 1970a). When $\psi = \tan^{-1}(\kappa_2/\kappa_1)$, there is no change in the normal stress across the fault during the slip.

Table 1 shows how $\Delta\tau/\Delta\sigma_1$ and $\Delta\sigma/\Delta\sigma_1$ vary with typical values of ψ and κ_2/κ_1. It is interesting that for certain combinations of ψ and κ_2/κ_1, the normal stress

Table 1

Resolved shear stress drop $\Delta\tau$ and normal stress drop $\Delta\sigma$ corresponding to observed drop in $\Delta\sigma_1$ as a function of fault orientation ψ and stiffness ratio κ_2/κ_1

κ_2/κ_1	ψ	$\Delta\tau/\Delta\sigma_1$*)	$\Delta\sigma/\Delta\sigma_1$*)
0	10°	0.171	0.030
	20	0.321	0.117
	30	0.433	0.250
	40	0.492	0.413
	45	0.500	0.500
	50	0.492	0.587
	60	0.433	0.750
0.50	10	0.186	−0.055
	20	0.379	−0.044
	30	0.558	0.033
	40	0.669	0.167
	45	0.750	0.250
	50	0.785	0.316
	60	0.808	0.533
1.00	10	0.201	−0.141
	20	0.438	−0.204
	30	0.683	−0.183
	40	0.905	−0.079
	45	1.00	0.00
	50	1.08	0.095
	60	1.183	0.317

*) A positive value means that a shear stress drop in the x direction ($\Delta\sigma_1$) is accompanied in a *drop* in shear stress ($\Delta\tau$), or normal stress ($\Delta\sigma$).

actually increases during the slip. For $\kappa_2/\kappa_1 = 1.0$, and $\psi = 45$; the normal stress across the fault does not change during slip.

Discussion

Table 2 gives values of some of the stick-slip parameters corresponding to different test techniques. However, it should be recognized that while Δs is independent of stiffness ratios, the angular frequency ω depends upon κ_1 and κ_2 independently. For convenience, the angular frequency ratio is introduced:

$$\frac{\omega(\kappa_2 \neq 0)}{\omega(\kappa_2 = 0)} = \sqrt{1 + \frac{\kappa_2}{\kappa_1}\mu_d^* \tan\psi} \tag{12}$$

From Table 2, it is seen that according to the model of Fig. 2b, the angular frequency ratio increases with stiffness ratio. The stress-drop ratio is of particular interest. It is

Table 2*)

Stick-slip parameters related to friction properties, stiffness and type of test

Friction parameters	Type of test	Fault orientation (See Fig. 3)	Stress drop $\Delta s/\sigma_0$	Peak stress ratio σ_1/σ_0 or τ/σ_0	Final stress ratio σ_1/σ_0 or τ/σ_0	Stiffness ratio κ_2/κ_1	Frequency ratio $\frac{\omega(\kappa_2 \neq 0)}{\omega(\kappa_2 = 0)}$
		30°	1.08	3.00	1.92	0.0	1.0
						0.5	1.16
	Triaxial					1.0	1.30
	and						
$\phi = 30°$	biaxial	45°	3.18	3.73	0.55	0.0	1.0
$\phi_d = 20°$						0.5	1.44
$i = 0°$						1.0	1.77
	Direct					for all	
	shear	0°	0.42	0.58	0.16	κ_2/κ_1	1.00
		30°	0.32	5.83	5.51	0.0	1.0
						0.5	1.11
	Triaxial					1.0	1.22
	and						
$\phi = 15°$	biaxial	45°	0.66	13.93	13.27	0.0	1.0
$\phi_d = 10°$						0.5	1.31
$i = 0°$						1.0	1.56
	Direct					for all	
	shear	0°	0.18	0.27	0.09	κ_2/κ_1	1.00

*) assumes μ_d is constant independent of κ_2.

strongly dependent on the fault inclination, and is independent of stiffness ratio. Yet SCHOLZ *et al.* found much smaller stress-drops in biaxial tests than did BYERLEE in triaxial tests for the same rock and fault inclination. This recalls the conundrum presented by small stress-drops of actual seismic events. We believe the problem lies partly with the assumption that μ_d is constant during slip and that there is no slip before full friction is mobilized, as noted with reference to Fig. 2c.

For example, Fig. 4 shows the path of hypothetical direct shear tests on rough fault surfaces with k_2 small (locus A-B-C) and k_2 large (locus A-D-E-F). The dynamic friction angle calculated from the kinetics of an instability in such a test cannot be smaller than the residual friction angle ϕ_r. If we assume $\phi_d = \phi_r$, then the stress drop, Δs will not be larger than

$$2\sigma_0[\tan(\phi_p + \psi) - \tan(\phi_r + \psi)] \tag{13}$$

Table 3 compares maximum stress-drops for the two paths in the hypothetical case for direct shear and triaxial tests.

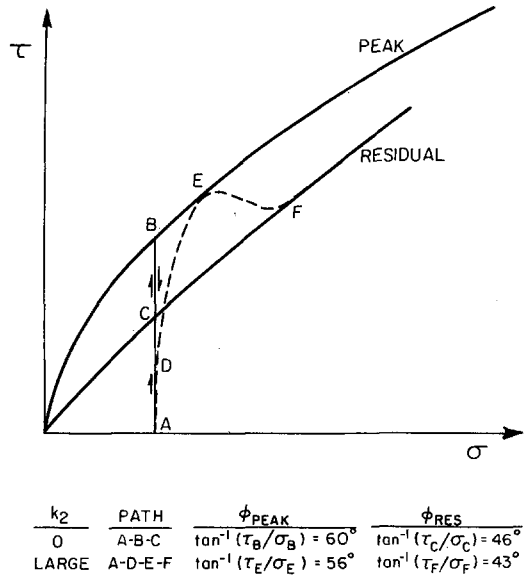

Figure 4
Stress path during direct shear on rough fault surfaces for small and large values of κ_2.

3. *Stiffness associated with a fault*

The model of Fig. 2b assumes that the stiffnesses of the fault itself are infinite. However, in the laboratory experiments and in the field, stick-slip is found to be preceded by some premonitory slip (e.g., LOGAN, 1975). Thus, one can introduce *fault shear stiffness* (k_s) and *fault normal stiffness* (k_n) (Fig. 5b). The values of k_s and k_n influence stick-slip phenomena because they reduce k_1 and k_2. Consider the direct shear test (with X parallel to the fault and $\psi = 0$). Because k_s is in series with k_1, the effective stiffness driving the slider in the X-direction is reduced from k_1 to $k_1/(1 + k_1/k_s)$. Similarly, the stiffness reacting in the Y-direction is reduced from k_2 to $k_2/(1 + k_2/k_n)$. Thus it is of interest to measure k_s and k_n for faults. The difficulty

Table 3
Effect of Stiffness on Δs *(Calculated using Fig. 3 (hypothetical case))*

Type of test	ψ	K_2	ϕ	ϕ_d	Maximum $\Delta s/\sigma_0$
Direct shear	0	0	60°	46°	1.39
Direct shear	0	large	56°	43°	1.10
Triaxial	25°	0	60°	46°	17.05
	25°	large	56°	43°	7.68

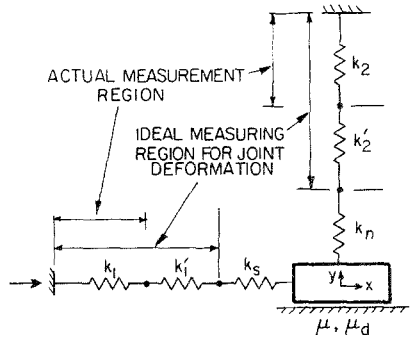

k_1, k_2 LOADING SYSTEM STIFFNESSES BETWEEN MEASURING POINT REFERENCE AND STATIONARY REFERENCE FRAME

k_1', k_2' STIFFNESSES IN MEASURED SYSTEM IN SERIES WITH FAULT

k_s, k_n TRUE STIFFNESSES OF THE FAULT

(a) GENERALIZED MODEL FOR LABORATORY TESTING OF FAULT SURFACES

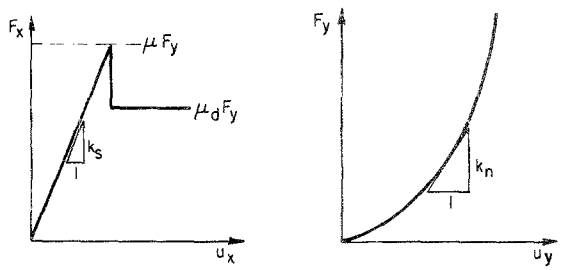

(b) SHEAR AND NORMAL STIFFNESSES OF THE FAULT

Figure 5
Direct shear of faults – influence of machine and measuring system.

with the measurement is indicated in Fig. 5a. The desired measurement of k_s is complicated by compliance in the material and fixtures holding the rock in the test device, e.g., the shear box, the wall-rock and the potting material. The displacement gage cannot be attached to the fault itself. Thus there is always the effect of a stiffness k_1' (Fig. 5a) in series with k_s in the fault shear displacement data. Similarly, the normal deformation experiment always includes apparatus stiffness k_2'. The influence of apparatus-stiffness is as follows: let the fault stiffness apparently measured be $k_{s,a}$; then the true value of k_s is

$$k_s = k_{s,a}/(1 - k_{s,a}/k_1') \tag{14}$$

and a similar expression for k_n

$$k_n = k_{n,a}/(1 - k_{n,a}/k_2')$$

Rosso (1976) has made fault stiffness measurements with k_1' and k_2' very large by using extensometers fixed near the fault surfaces.

4. *Stiffness for a fault slipping over a finite length*

An actual fault-motion initiates at a point or over a small segment of length bounded between locked regions. This occurs also in laboratory direct shear and triaxial experiments but the rupture quickly propagates to the extremities of the specimen. In a biaxial experiment with a large specimen the rupture propagation may take a considerably longer time. For conditions of a growing dislocation, the stiffnesses of the surrounding rock could be calculated using the theory for an open crack in an infinite elastic medium (NEVILLE COOK, personal communication). The resulting stiffnesses vary inversely with the fault length, with implications for gradual development of an instability through fault extension.

Using a plane strain solution for displacements in an infinite region with an elliptical crack (JAEGER and COOK, 1976, Sections 10–11), the stiffness of the adjacent rock parallel and perpendicular to the crack (κ_a and κ_b respectively – see Fig. 3e) are found to be

$$\kappa_a = \kappa_b = \frac{E}{2(1 - \nu^2)l} \tag{15}$$

where l is the length of the fault undergoing slip and E and ν are respectively the Young's modulus and Poisson's ratio of the surrounding rock.[5]) A similar result can be derived from solutions for a penny-shaped crack (SNEDDON, 1946; SEGEDIN, 1951; KEER, 1966; and WALSH, 1971). For a penny-shaped crack also, $\kappa_b \approx \kappa_a$.[5]) Note that the shear stiffness for out-of-plane shear is $\kappa_a/(1 + \nu)$.

If we assume $\kappa_a = \kappa_b$, the system is isotropic and $\kappa_1 = \kappa_2$ regardless of ψ. In this respect, a natural fault would behave unlike a triaxial compression specimen under constant normal stress for it is confined with a stiffness ratio of unity.

Moreover, both κ_1 and κ_2 vary inversely with l so the stiffness of the 'loading mechanism' declines as the disturbance propagates. PRATT *et al.* (1974) also noted an inverse relation between stiffness and length. The implications are suggested in Fig. 6. Consider a fault surface undergoing stable sliding under constant normal stress, i.e. $\kappa_2 = 0$. Friction fluctuates up and down during stable sliding due to the formation

[5]) The more precise expressions are

$$k_a = \frac{\Pi}{8} \frac{2 - \nu}{1 - \nu} G a$$

where a is the radius and $G = [E/2(1 + \nu)]$ and

$$k_b = \frac{\Pi}{4} \frac{G}{(1 - \nu)} a$$

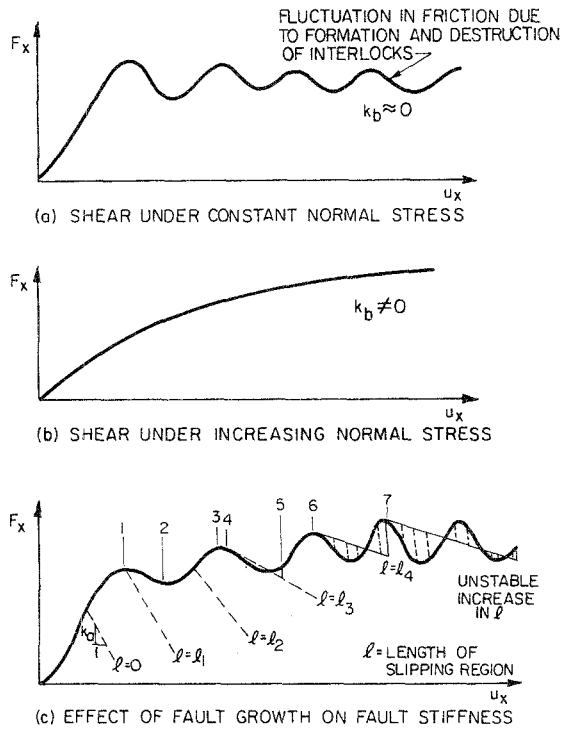

Figure 6

Implications on sliding behavior of decreasing stiffness with increasing fault length.

0–1 Fault creep with stress build-up
1–2 Fault creep with stress relaxation
2–3 Fault creep with stress build-up
3–4 Fault creep with stress relaxation
4–5 Foreshock
5–6 Stress build-up without creep followed by stress build-up with creep
6–7 Large foreshock
7→ Stress build-up without creep followed by earthquake

and destruction of interlocks and bridges. If the same surface undergoes sliding with $\kappa_2 = \kappa_1$, the normal stress will gradually increase. Similarly, if slip initiates over a short segment of a locked fault, with $\kappa_2 = \kappa_1$, then the normal stress will begin to increase and, since κ_2 varies with l in an inverse manner, the rate of increase of σ will decline with displacement, yielding the type of curve shown in Fig. 6b. As a result, the fluctuations of friction with sliding will augment as shown in Fig. 6c. Initially, κ_1 is large and stable sliding (creep) prevails. But as the slip region lengthens and κ_1 decreases, larger and larger instabilities occur, liberating foreshocks and finally a major earthquake. It should be possible to examine this scenario through appropriate friction tests, in direct shear or biaxial mode, using large specimens and rough or gouge-covered surfaces.

5. Conclusions

Sliding phenomena of fault surfaces are strongly influenced by testing techniques. The common testing techniques, triaxial, direct shear, double shear and biaxial shear, have different system stiffnesses and employ different orientations of fault surface with respect to loading directions. For rough faults in direct shear the stiffnesses of both the shear load and the normal load mechanisms affect dynamic instability. For smooth faults in direct shear the normal load stiffness has less of an effect on stick-slip. However, in triaxial and biaxial tests, even for smooth faults, both X and Y stiffnesses (k_1 and k_2, Fig. 3) affect stick-slip.

In a triaxial system, where k_2 is usually much smaller than k_1, a drop of normal stress during slip occurs for all workable inclinations of the fault. On the other hand, in a biaxial test mode where k_1 is essentially equal to k_2, shear stress drop occurs under essentially constant normal stress for the fault inclination of 45°.

Be it the laboratory or the field a fault can be assigned finite stiffnesses, k_n across and k_s along the surfaces of contact (Fig. 5). These values are particularly important in understanding stable sliding as well as the dynamic instability of faults. However, they are not easily measured even under laboratory conditions. The influence of fault stiffnesses on dynamic instability has apparently been neglected.

For a fault which is a growing dislocation, it can be shown that both the normal and shear stiffnesses of the wall-rock are the same and decrease with increasing length of fault. The application of such a model is apparent in Fig. 6. Such a model may easily explain the occurrence of pre-seismic creep, stick, and foreshocks, before the final earthquake.

6. Acknowledgements

The authors benefited from illuminating discussions with Dr. Neville Cook, who suggested the model for equation (15) and Fig. 6. The comments of Dr. James Byerlee, Professor William Brace, and Professor John Handin at an embryonic stage and those of an anonymous reviewer were helpful.

References

BRACE, W. F. and BYERLEE, J. D. (1966), *Stick-slip as a mechanism for earthquakes*, Science *153*, 990–992.

BYERLEE, J. D. and BRACE, W. F. (1968), *Stick-slip, stable sliding, and earthquakes – Effect of rock type, pressure, strain rate and stiffness*, J. Geophys. Res. *73*, 6031–6037.

BYERLEE, J. D. (1970a), *Static and kinetic friction of granite at high normal stress*, Int. Jour. Rock Mech. Min. Sci. *7*, 577–582.

BYERLEE, J. D. (1970b), *The mechanics of stick-slip*, Tectonophysics *9*, 475–486.

HANDIN, J. and STEARNS, D. W. (1964), *Sliding friction of rock*, Trans. Am. Geophys. Un. *45*, 103.

JAEGER, J. C. and COOK, N. G. W., *Fundamentals of rock mechanics* (Chapman and Hall, London, 1976).

KEER, L. M. (1966), *A note on shear and combined loading for a penny-shaped crack*, Jour. The Mech. and Phys. of Solids *14*, 1–6.

LOGAN, J. M. (1975), *Friction in rocks*, Rev. of Geophys. and Space Phys. *13*, 358.

OBERT, L., BRADY, B. T. and SCHMECHEL, F. W. (1976), *The effect of normal stiffness on the shear resistance of rock*, Rock Mechanics, *8*, 57.

PRATT, H. R., BLACK, A. D. and BRACE, W. F. (1974), *Friction and deformation of jointed quartz diorite*, 3rd Int. Cong. Int. Soc. Rock Mech., V. *II*, 306.

ROSSO, R. S. (1976), *A comparison of joint stiffness measurements in direct shear, triaxial compression and in-situ*, Int. Jour. Rock Mech. Min. Sci. *13*, 167–172.

SCHOLZ, C., MOLNAR, P. and JOHNSON, T. (1972), *Detailed studies of frictional sliding of granite and implications for earthquake mechanism*, J. Geophys. Res. *77*, 6392–6406.

SEGEDIN, C. M. (1951), *Note on a penny-shaped crack under shear*, Camb. Phil. Soc. 47, *2*, 396–400.

SNEDDON, I. N. (1946), *The distribution of stress in the neighbourhood of a crack in an elastic solid*, Proc. Roy. Soc. London, *187*, 229–260.

TOLSTOI, D. M. (1967), *Significance of the normal degree of freedom and natural normal vibrations in contact friction*, Wear *10*, 199–213.

WALSH, J. B. (1971), *Stiffness in faulting and in friction experiments*, J. Geophys. Res. *76*, 8597–8598.

WELLS, J. H. (1929), *Kinetic boundary friction*, Engineer (London) *147*, 454.

(Received 6th June 1977)